Supporting Information for:

Effect of Sampling Rate and Data Pretreatment for Targeted and Nontargeted Analysis by Means of Liquid Chromatography Coupled to Drift Time Ion Mobility Quadruple Time-of-Flight Mass Spectrometry

Kristina Tötsch, [†‡] John C. Fjeldsted, [§] Sarah M. Stow, [§] Oliver J. Schmitz, [†‡] Sven W. Meckelmann[†‡]

[†] Applied Analytical Chemistry, University of Duisburg-Essen, Universitätsstrasse 5, 45141 Essen, Germany

[‡] Teaching and Research Center for Separation, University of Duisburg-Essen, Universitätsstrasse 5, 45141 Essen, Germany

[§] Agilent Technologies, Santa Clara, California, USA

Corresponding author: Sven W. Meckelmann - Applied Analytical Chemistry, University of Duisburg-Essen, Universitätsstrasse 5, 45141 Essen, Germany https://orcid.org/0000-0002-0407-7879 E-mail: sven.meckelmann@uni-due.de

Content

1 Additional Information on lipid extraction and analysis parameters

Lipid extraction protocol

LC-MS grade isopropanol and methanol as well as GC grade chloroform and n-hexane were obtained from VWR International (Darmstadt, Germany). LC-MS grade acetic acid was purchased from Merck (Darmstadt, Germany). Deuterated 12-Hydroxyeicosatetraenoic acid (12-HETE-$^{2}H_{8}$) and arachidonic acid (AA-$^{2}H_{8}$) were from Cayman Chemicals (local distributor: Biomol, Hamburg, Germany). SPLASH® LIPIDOMIX® Mass Spec Standard was purchased from Avanti Polar Lipids (local distributor: Sigma Aldrich, Steinheim, Germany). Ultrapure and desalted water with a resistivity of 18.2 M Ω/cm was generated by a Sartorius Stedim water purification system (Sartorius, Goettingen, Germany).

For all biological matrices, the same protocol for lipid extraction was used. 15 µL plasma or serum was combined with 185 µL water, 1 µL acetic acid and 10 µL internal standard (SPLASH® LIPIDOMIX® Mass Spec Standard spiked with 12-HETE-$^{2}H_{8}$ and AA-$^{2}H_{8}$, final concentrations of all deuterated standards in the extracts are listed in Table S2) 500 µL of solvent (1M acetic acid/isopropanol/hexane; 2:20:30; v/v/v) was added to the samples. After vortexing for 1 min 500 µL hexane was added, vortexed again for 1 min, centrifuged for 10 min at 200 g. The upper hexane layer was collected, while the lower aqueous layer was re-extracted. Therefore, 500 µL hexane was added, vortexed for 1 min, and centrifuged for 10 min at 200 g. The upper hexane layer was collected and combined with the first hexane layer. A modified Bligh and Dyer protocol was used for another re-extraction of the remaining aqueous phase.[1] First, 750 µL chloroform/methanol; 1:2; v/v was added to the samples and vortexed for 1 min. Second, 250 µL chloroform was added and again vortexed for 1 min. Third, 250 µL water was added to induce phase separation and vortexed for 1 min. Finally, the samples were centrifuged for 10 min at 200 g and the bottom chloroform layer was collected and combined with the two hexane layers. The combined extracts were dried under vacuum and re-suspended in 80 µL methanol. The final extracts were divided into 40 µL aliquots and stored in two HPLC-vials for analysis in ESI positive and negative mode at -80 °C until analysis.
For HepG2 cells 10^{6} cells were suspended in 200 µL water and given to a mixture of 1 µL acetic acid, 10 µL internal standard and 500 µL of solvent (1M acetic acid/isopropanol/hexane; 2:20:30; v/v/v). The cell samples were re-suspended in 100 µL methanol. All other steps remained as described before.

Additional IM parameters

Table S1: Additional IM parameters

Parameter	Value
Drift tube entrance voltage (V)	1700
Drift tube exit voltage (V)	250
Drift gas	Nitrogen
Drift gas pressure (Torr)	3.950
HP funnel voltage (V)	(delta) 150
Trap funnel voltage (V)	(entrance) 91
Rear funnel voltage (V)	240

CCS calibration

CCS values were calculated by single field calibration method as described by Gabelica et al.[2]. For this, the same ion source conditions as for the analysis of all other samples were used to monitor the masses of the calibration Mix (Agilent ESI TuneMix) for 1 min. In the positive ionization mode, the calculated β-value was 0.129 and T_{fix} -0.151, In the negative ionization mode, the calculated values for Beta was 0.130 and for T_{fix} -0.239.

2 Additional results

2.1 Method characterization

Deuterated lipid standards from different lipid classes were analyzed. Extracted ion chromatograms as heat maps are shown in Figure S1. We use the abbreviations and nomenclature for lipids according to LIPID MAPS[3]. The standards were spiked to five human blood plasma samples before and to five extracts after extraction. The data was used to determine peak widths, the reproducibility of retention times, peak areas, CCS values, and *m/z* values in matrix as well as extraction recovery (Table S2 and Figure S2). Further, three lipid extracts of human blood serum and HepG2 cells were spiked to investigate ion suppression effects in different matrices (Figure S3 and S4). In addition, a dilution series was prepared in methanol, and limits of detection (LOD) and quantification (LOQ) were determined using the 3σ method based on Kaiser and Specker[4] (Table S3 and S4).

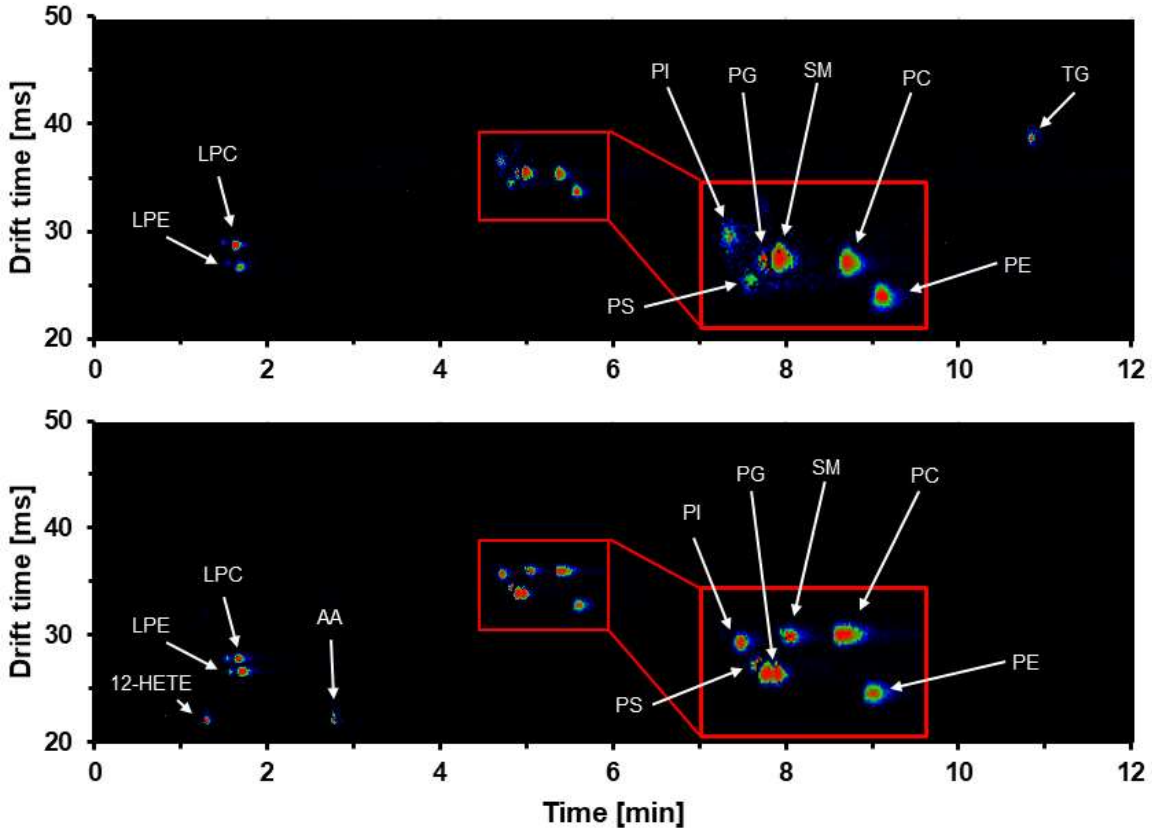

Figure S1: Extracted ion chromatograms as heat maps of an LC-IM-qTOF-MS analysis. Standards were separated by reversed-phase chromatography using a Waters Acquity UPLC CSH C18 (100 x 2.1 mm; 1.7 µm) and detected by IM-qTOF-MS in alternating frame mode. Top: mass traces for lipid ions from Table S3 in ESI positive mode. Bottom: mass traces for lipid ions from Table S4 in ESI negative mode.

Table S2: Method performance parameters of the described LC-IM-qTOF-MS method using 2 summed transients for deuterated lipid standards spiked to human blood plasma before the lipid extraction (n = 5). All standards were spiked in a concentration range that is typical for the physiological concentration of this lipid class in human blood plasma.

Lipid	Adduct	Concen-tration [nmol/L]	Peak area		Retention time		FWHM* [min]	CCS		Observed m/z	mass error [ppm]
			Mean [AU]	Rel. SDev. [%]	Mean [min]	Rel. SDev. [%]		Mean [Å²]	Rel. SDev. [%]		
PC(15:0/18:1($^2H_7$))	$[M+H]^+$	23,597	3,451,765	3.60	5.446	0.15	0.130	284.07	0.02	753.6175	5.51
PE(15:0/18:1($^2H_7$))	$[M+H]^+$	895	74,256	4.39	5.626	0.24	0.076	269.87	0.04	711.5655	-1.30
PS(15:0/18:1($^2H_7$))	$[M+H]^+$	592	20,039	13.84	4.890	0.34	0.066	276.83	0.12	755.5534	-3.74
LPC(18:1($^2H_7$))	$[M+H]^+$	5,312	781,507	3.51	1.696	0.29	0.068	232.17	0.05	529.3990	-0.59
LPE(18:1($^2H_7$))	$[M+H]^+$	1,188	24,952	4.20	1.744	0.58	0.046	215.85	0.12	487.3536	2.42
TG(15:0/18:1($^2H_7$)/15:0)	$[M+NH4]^+$	7,670	645,098	7.82	10.898	0.07	0.078	310.55	0.07	829.7986	0.13
SM(d18:1/18:1($^2H_9$))	$[M+H]^+$	4,732	967,957	3.67	5.072	0.08	0.090	286.61	0.03	738.6496	3.53
PC(15:0/18:1($^2H_7$))	$[M+CHO_2]^-$	23,597	1,090,792	5.14	5.446	0.15	0.110	287.45	0.04	797.6050	0.86
PE(15:0/18:1($^2H_7$))	$[M-H]^-$	895	196,655	8.74	5.640	0.16	0.070	262.62	0.03	709.5502	-2.32
PS(15:0/18:1($^2H_7$))	$[M-H]^-$	592	50,193	8.28	4.876	0.40	0.082	272.96	0.02	753.5425	1.01
PG(15:0/18:1($^2H_7$))	$[M-H]^-$	4,124	1,405,344	5.13	4.956	0.10	0.072	269.81	0.02	740.5508	5.93
PI(15:0/18:1($^2H_7$))	$[M-H]^-$	1,184	135,050	3.57	4.774	0.10	0.074	283.98	0.03	828.5667	5.08
LPC(18:1($^2H_7$))	$[M-CH_3]^-$	5,312	311,109	8.78	1.702	0.24	0.068	222.73	0.02	513.3738	9.06
LPE(18:1($^2H_7$))	$[M-H]^-$	1,188	133,244	8.29	1.742	0.23	0.056	214.21	0.04	485.3362	-3.32
SM(d18:1/18:1($^2H_9$))	$[M+CHO_2]^-$	4,732	25,396	7.98	5.096	0.27	0.094	288.14	0.07	782.6372	-0.97
12-HETE($^2H_8$)	$[M-H]^-$	1,796	114,930	7.23	1.328	0.56	0.048	181.41	0.05	327.2778	-0.93
AA($^2H_8$)	$[M-H]^-$	3,776	15,094	5.09	2.806	0.36	0.046	181.99	0.13	311.2830	-0.67

*Full width at half maximum

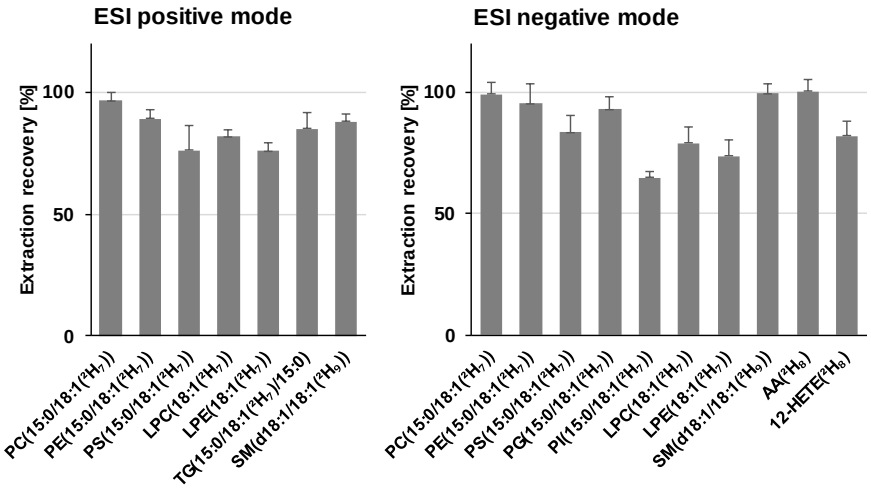

Figure S2: Recoveries for the deuterated lipid standards spiked in human blood plasma. For the determination of the recoveries, the deuterated lipid standards were spiked to human blood plasma (n = 5) before and after extraction and the obtained peak areas after the analysis by LC-IM-qTOF-MS were compared. The recovery of all lipids ranged from 60 to 110%.

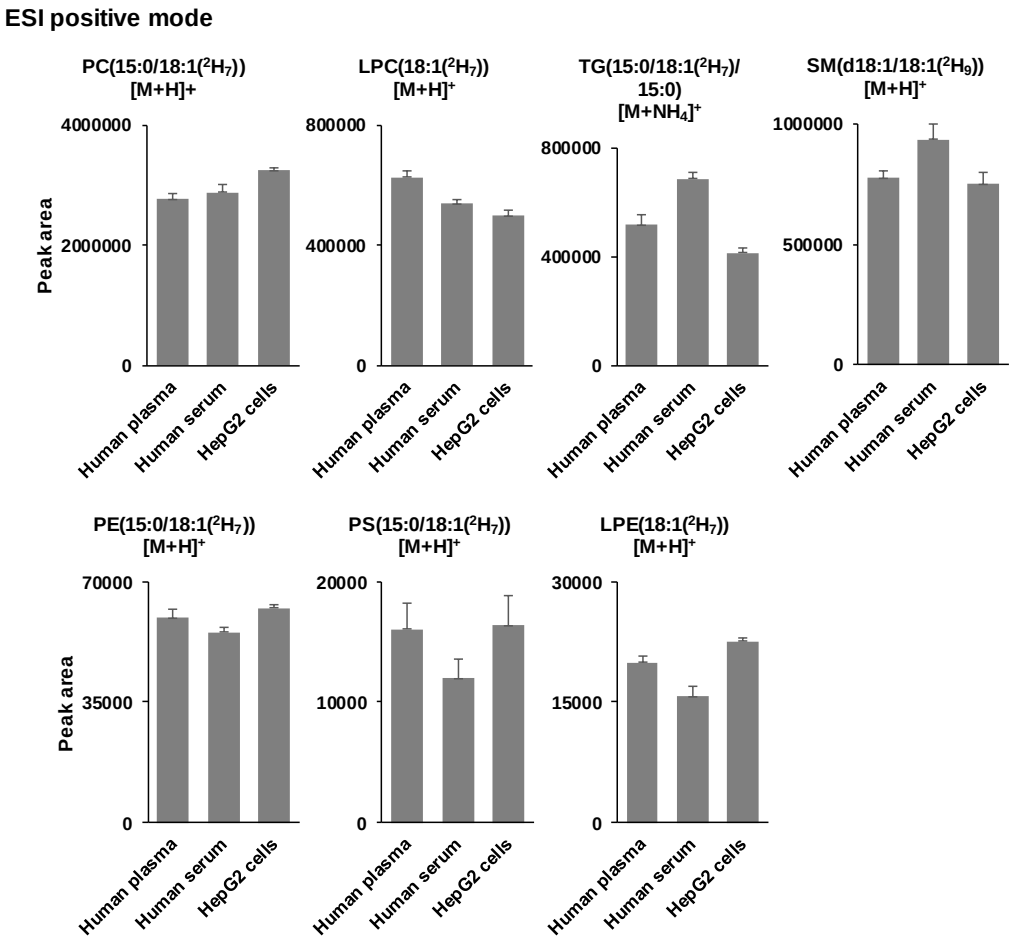

Figure S3: Peak areas of deuterated lipid standards in lipid extracts of different biological samples (human blood plasma, human blood serum, and HepG2 cells, n = 3) analyzed by LC-IM-qTOF-MS in positive ESI mode. All peak areas of the investigated lipids are in a similar range. However, some differences between the matrices were found, which can be attributed to matrix effects such as ion suppression.

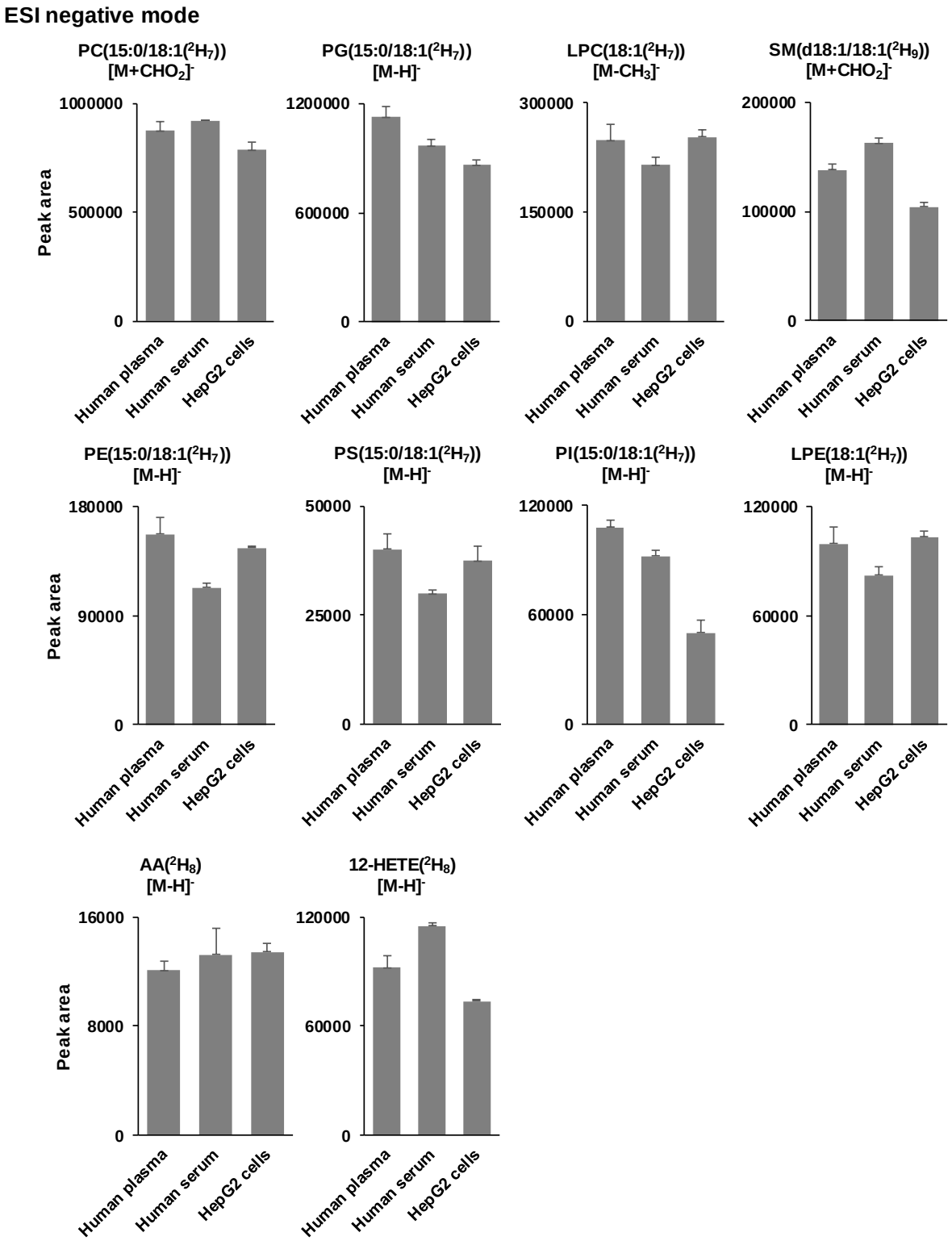

Figure S4: Peak areas of deuterated lipid standards in lipid extracts of different biological samples (human blood plasma, human blood serum and HepG2 cells, n = 3) analyzed by LC-IM-qTOF-MS in negative ESI mode. All peak areas of the investigated lipids are in a similar range. However, some differences between the matrices were found, which can be attributed to matrix effects such as ion suppression.

The LODs and LOQs are presented in Tables S3 and S4. Comparing these results with lipid concentrations reported for the SRM 1950 NIST Plasma (Metabolites in Frozen Human Plasma)[5] shows that LODs and LOQs of the presented method allow the detection of relevant differences across a broad range of major lipid classes in biological samples. In detail, LODs of the triglyceride-, sphingomyelin- and all glycerophospholipid standards, except the PA(15:0/18:1($^2H_7$)), were between 18 and 95 nmol/L, while LOQs were between 57 and 284 nmol/L. All concentrations of the triglycerides, sphingomyelins, PGs, PIs, PEs, and LPEs, quantified in the study[5] were above the determined LOQs using the deuterated lipid standards for different lipid classes. Furthermore, the concentrations of all 53 reported PCs were above the determined LOD of 19 nmol/L for PC(15:0/18:1($^2H_7$)), while only two PCs were below the LOQ of 57 nmol/L. Four of 25 LPCs had a concentration under the determined LOQ of 127 nmol/L. Out of these, two concentrations lay under the LOD (42 nmol/L), which are LPC(22:0) and LPC(22:1) with concentrations of 25 and 13 nmol/L, respectively. The inter-laboratory study reported concentrations of only five free fatty acids and three eicosanoids. All concentrations of the free fatty acids were above the determined LOD of AA($^2H_8$) of 302 nmol/L, while four were also above the LOQ of 906 nmol/L.

Table S3: Limits of detection (LOD) and quantification (LOQ) of deuterated lipid standards analyzed by LC-IM-qTOF-MS in ESI positive mode determined by the 3σ method based on Kaiser and Specker[4].

Lipid	Adduct	LOD [nmol/L]	LOD [ng/mL]	LOD [fmol on column]	LOQ [nmol/L]	LOQ [ng/mL]	LOQ [fmol on column]
PC(15:0/18:1($^2H_7$))	$[M+H]^+$	19	14	38	57	43	113
PE(15:0/18:1($^2H_7$))	$[M+H]^+$	21	15	43	72	50	143
PS(15:0/18:1($^2H_7$))	$[M+H]^+$	142	110	284	474	368	948
PG(15:0/18:1($^2H_7$))	$[M+H]^+$	990	756	1,979	3,299	2,519	6,598
PA(15:0/18:1($^2H_7$))	$[M+NH_4]^+$	2,832	1,953	5,664	9,441	6,509	18,882
LPC(18:1($^2H_7$))	$[M+H]^+$	42	22	85	127	67	255
LPE(18:1($^2H_7$))	$[M+H]^+$	95	46	190	285	139	570
CE(18:1($^2H_7$))	$[M+NH_4]^+$	14,163	9,314	28,326	47,210	31,047	94,419
DG(15:0/18:1 ($^2H_7$))	$[M+NH_4]^+$	4,239	2,491	8,478	14,130	8,302	28,259
TG(15:0/18:1($^2H_7$)/ 15:0)	$[M+NH_4]^+$	18	15	37	61	50	123
SM(d18:1/18:1($^2H_9$))	$[M+H]^+$	38	28	76	114	84	227

Table S4: Limits of detection (LOD) and quantification (LOQ) of deuterated lipid standards analyzed by LC-IM-qTOF-MS in ESI negative mode determined by the 3σ method based on Kaiser and Specker[4].

Lipid	Adduct	LOD [nmol/L]	LOD [ng/mL]	LOD [fmol on column]	LOQ [nmol/L]	LOQ [ng/mL]	LOQ [fmol on column]
PC(15:0/18:1($^2H_7$))	$[M+CHO_2]^-$	189	142	944	566	426	2,832
PE(15:0/18:1($^2H_7$))	$[M-H]^-$	21	15	107	72	50	358
PS(15:0/18:1($^2H_7$))	$[M-H]^-$	47	37	237	142	110	711
PG(15:0/18:1($^2H_7$))	$[M-H]^-$	33	25	165	99	76	495
PI(15:0/18:1($^2H_7$))	$[M-H]^-$	95	80	474	284	241	1,421
PA(15:0/18:1($^2H_7$))	$[M-H]^-$	944	651	4,720	2,832	1,953	14,161
LPC(18:1($^2H_7$))	$[M-CH_3]^-$	127	67	637	425	225	2,125
LPE(18:1($^2H_7$))	$[M-H]^-$	29	14	143	95	46	475
SM(d18:1/18:1($^2H_9$)	$[M+CHO_2]^-$	38	28	189	114	84	568
12-HETE($^2H_8$)	$[M-H]^-$	43	14	216	144	47	718
AA($^2H_8$)	$[M-H]^-$	302	94	1,510	906	283	4,531

2.2 Calibration curves for different IM-transient sums

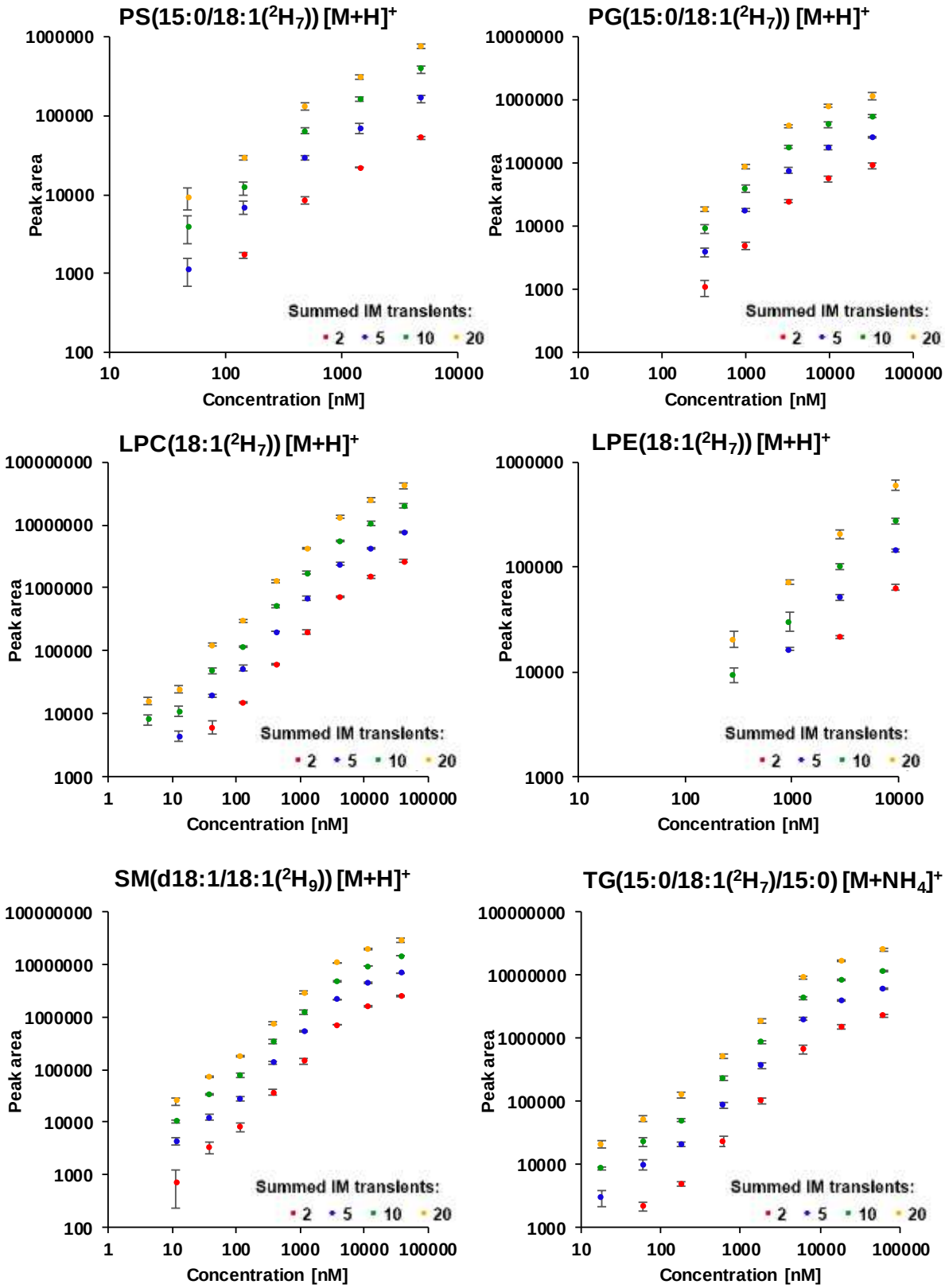

Figure S5: Calibration curves for deuterated lipid standards at different IM-transient sums analyzed by LC-IM-qTOF-MS in ESI positive mode. All solutions were prepared freshly prior to the analysis in LC-MS grade methanol. Each dilution was analyzed three times (n=3).

2.3 Effect of data preprocessing on the chromatographic resolution

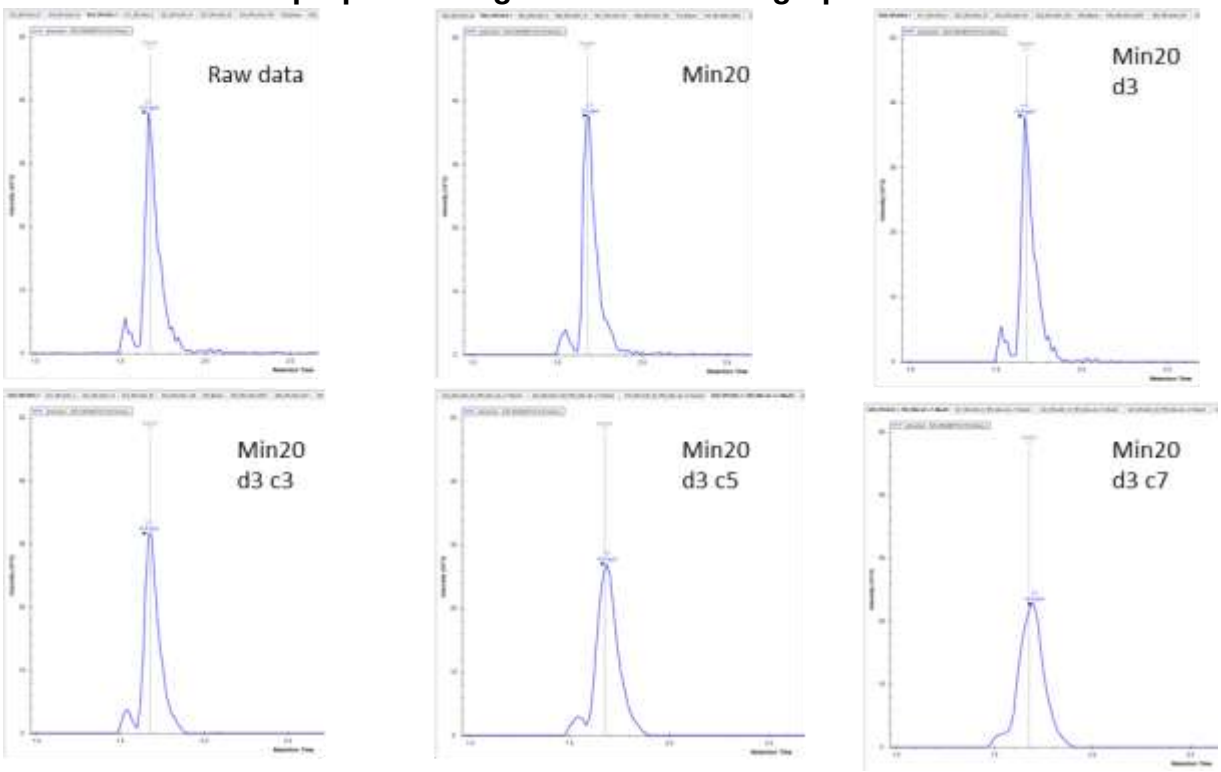

Figure S6: EICs of the LPC(18:1($^2H_7$))-$[M+H]^+$ ion at a concentration of 425 nM and a threshold of 20 counts (Min20) below which data points are removed. In addition, a moving average was used for smoothing. First, solely over three points in the drift dimension (d3), second, over three points in the drift dimension, and additionally over three, five, and seven points in chromatography (d3 c3, d3 c5, and d3 c7). Smoothing results in smaller and broader peaks, causing a loss of resolution. Starting with smoothing over five points, the two peaks, which were previously baseline separated, are merged.

2.4 Details on feature analysis

Optimization of alignment parameters

The software searches for features in each data file individually. Afterwards, the features are compared and combined, if they belong to the same compound. The alignment parameters specify in which range (chromatography, drift, and *m/z* dimension) the features of different measurements are combined to one feature. If the alignment parameters are chosen too small, several features with low frequencies will result for one compound, because they cannot be combined. If the parameters are too large, features of different compounds may be combined into one feature, i.e. the separation performance of the method decreases. Figure S7 shows the number of features obtained in a feature analysis of three lipid extracts from HepG2 cells at different alignment parameters. Initially, relatively small parameters were chosen (mass tolerance: 10 ppm, drift time tolerance = 1.5%, and retention time tolerance = 0.15 min) and then successively increased. Thereby, a decrease in the total number of features and an increase in the number of features with high frequencies is an indication that the original alignment parameters were chosen too small. In the example shown, increasing the drift time tolerance from 1.5% to 2.5% does not result in a significant difference. Increasing the mass tolerance from 10 ppm to 20 ppm results in a slight increase in the number of features with a frequency of two by ten features while decreasing the number of

features with a frequency of one by 18 features. A slightly larger effect can be observed when the retention time tolerance is increased. If the retention time tolerance is increased from 0.15 to 0.3 min, 19 additional features with a frequency of three are found and 38 less with a frequency of one. Increasing the retention time tolerance from 0.15 to 0.5 min results in a larger effect: 36 additional features with a frequency of three are found and 65 less with a frequency of one. However, a retention time tolerance above 0.3 min is critical because the observed half-widths ranged from 0.4 to 0.15 min and the deviation between measurements was less than 1%. The larger the tolerance, the greater the likelihood that features that actually belong to different components will be falsely grouped.

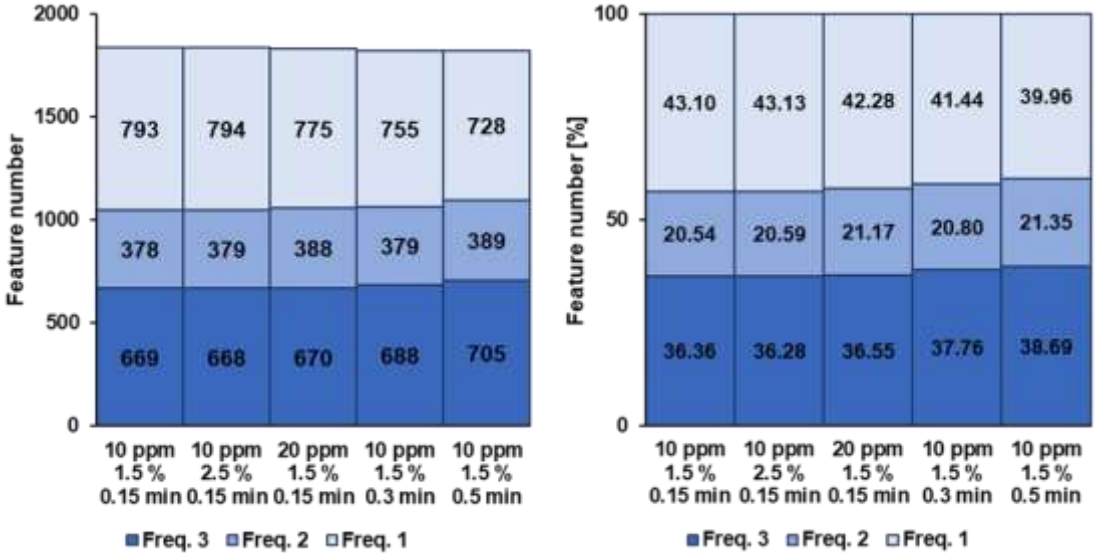

Figure S7: Feature analyses of three lipid extracts of HepG2 cells analyzed by LC-IM-qTOF-MS were performed. The alignment parameters (mass, drift, and retention time tolerances in which found features are combined into one) were varied and the obtained feature numbers were plotted according to their frequency. A decrease in the number of features found with an increase in the number of features with a frequency of three may be an indication that the alignment parameters were chosen too small. Increasing the tolerances had only a small impact. Only by increasing the retention time tolerance, additional features with a frequency of three could be found, while the number of features with a frequency of one decreased.

Influence of feature analysis parameters on feature numbers

To reduce the number of false-positive features, different filters can be used. Examples include abundance filters or frequency filters which require features to be reported in replicate samples. Another possibility is to use a score that evaluates the features on different criteria. The Mass Profiler was used in this study for the feature analysis, provides the Q-Score which evaluates peak shapes and if isotopic ions share the chromatographic profile. Furthermore, single ion features (features without detected isotopic pattern) can be reported with a charge state of z = 1 or excluded from the analysis. All these filters increase the reliability of features and can minimize the number of false-positive features. On the other hand, filters also increase the possibility of excluding compounds from the analysis. For example, some lipid classes do not have a Gaussian peak shape, isotopic patterns can be overlaid by other compounds or they would be missed for low abundant compounds, especially if they have a low molecular weight.

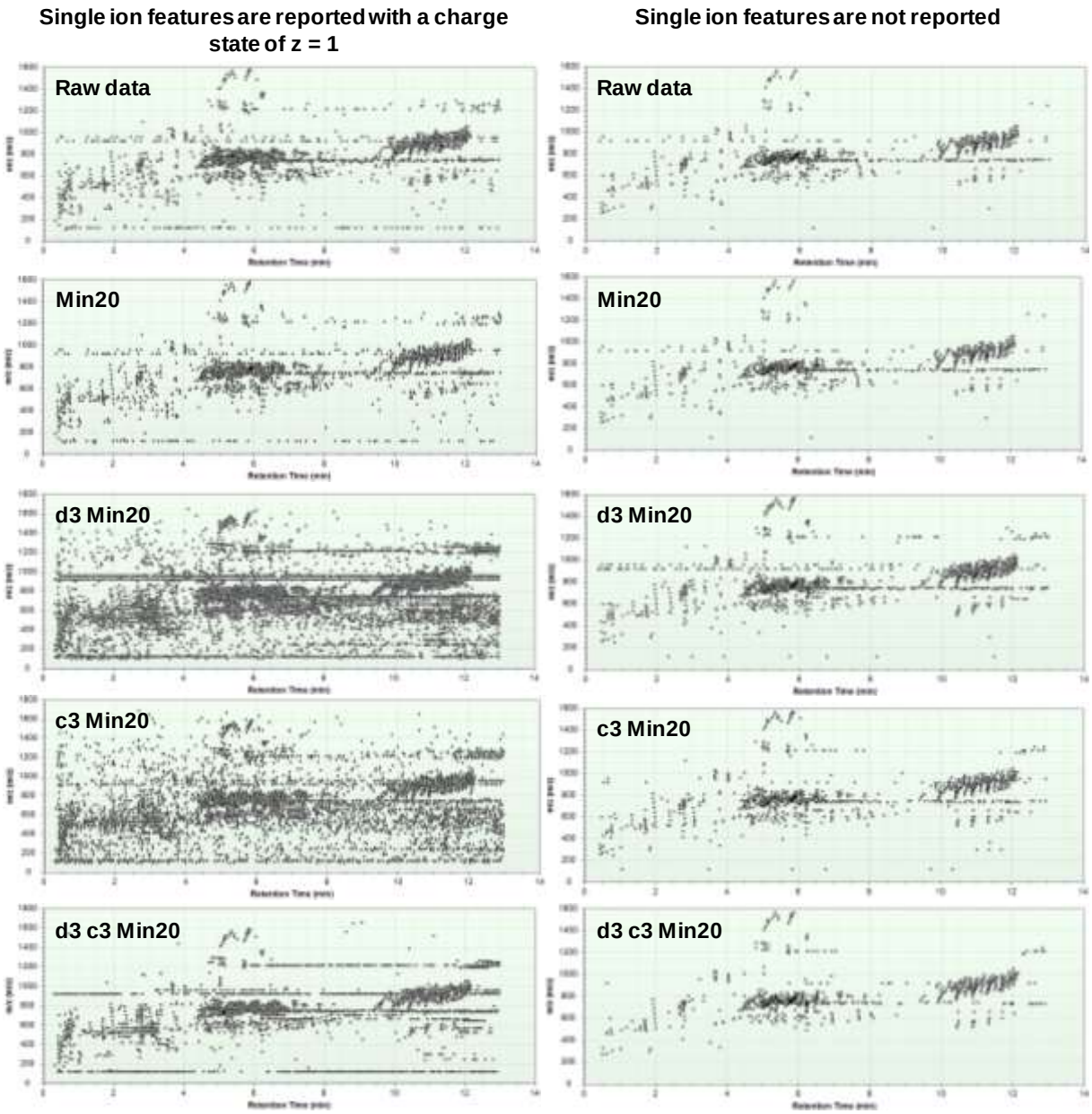

Figure S8: Three lipid extracts of HepG2 cells were analyzed by LC-IM-qTOF-MS. Feature analysis was performed after different data pretreatment. Ion maps (*m/z* value vs. retention time plots) are shown to illustrate the influence of data pretreatment on the found features. Left: single ion features are reported with a charge state of z = 1. Right single ion features are not reported. For a threshold of 20 counts (Min20) only minor effects were observed. Additional smoothing average over 3 points in drift (Min20 d3) or chromatographic dimension leads to a strong increase of features if single ion features are reported. These features are found over the whole chromatographic and *m/z* range. This supports the thesis, that false positive peaks are formed due to smoothing. Since these peaks originate from background noise they will occur everywhere. If smoothing average is also applied over 3 points in chromatography (Min20 d3 c3) feature number reduces to the initial count.

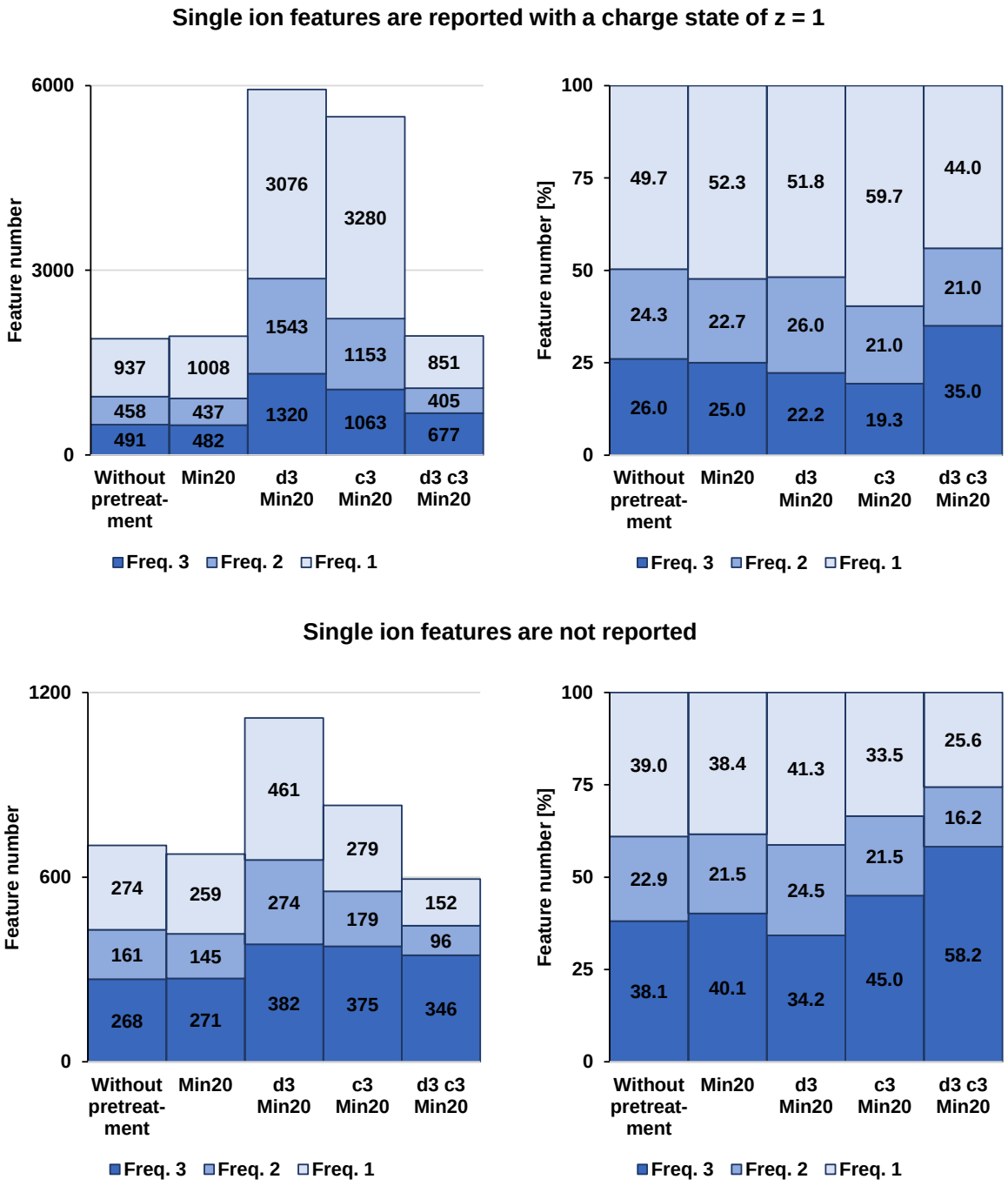

Figure S9: Feature analyses of three lipid extracts of HepG2 cells analyzed by LC-IM-qTOF-MS were performed with different feature analysis and data pretreatment parameters. **Top:** single ions are reported with a charge state of z = 1. **Bottom:** single ions were not reported. Found features are plotted by their frequency in absolute (**left**) and relative numbers (**right**). For data pretreatment, all data points below a threshold of 20 were removed (Min20), in addition, a simple moving average was performed over three points in the drift (d3 Min20), in the chromatographic (c3 Min20), and in the drift and chromatographic dimension (d3 c3 Min20). If single ion features are not reported, feature numbers decrease notably. In both cases, most features are reported for d3 Min20 and c3 Min20. This might be caused by the formation of false positive peaks due to the smoothing. The effect is larger for the lower quality condition which allows single ions to be reported with a charge state of z = 1, consistent with relatively more features with a frequency of 1 are reported: over 10 percentage points more for d3 Min20 and over 25 percentage points more for c3 Min20. If false positive peaks are formed due to smoothing, they are more likely to occur randomly in all data files at different m/z ratios as well as drift

and retention times. In addition, they would unlikely have an isotopic pattern. Therefore, they would only be reported as single ion features. For d3 c3 Min20 the total as well as the relative number of features with a frequency of three increases in both cases. If single ion features are not reported the relative number of features with a frequency of three is much higher with 58.2% compared to 35.0%, but the absolute number nearly halves. Single ion features have a higher possibility of being false positives and are less reliable, but there is also a high possibility to exclude compounds from the feature analysis by not reporting them. Therefore, parameters must be chosen carefully.

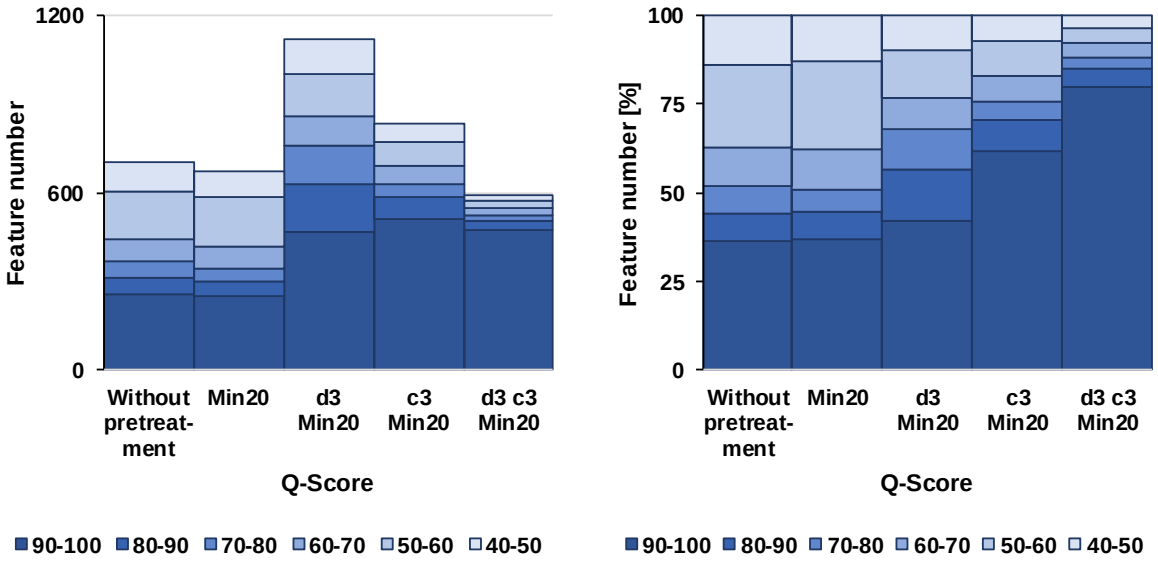

Figure S10: Feature analyses of three lipid extracts of HepG2 cells analyzed by LC-IM-qTOF-MS were performed with different data pretreatment parameters. Feature numbers are shown in absolute (**left**) and relative numbers (**right**) and are plotted by their Q-Score. If data points below a threshold of 20 were removed (Min20) no big influence could be observed. As discussed in the main article total number of reported features increases for smoothing in only drift (d3 Min20) or chromatographic dimension (c3 Min20) and decreases again for smoothing in both dimensions (d3 c3 Min20), which can be explained by the formation of false positive peaks. The relative numbers show that smoothing strongly increases the Q-Score of the reported features. For d3 c3 Min20 80% have a Q-Score over 90 compares to only 30% without smoothing. This results from the fact that the Q-Score includes the evaluation of peak shapes, that improve due to the smoothing.

Example for combined features

Figure S11 shows an example found in the data for a case where the features of a component are only accurately combined by data pretreatment. The mass peaks integrated are highlighted in purple. The isotopic peaks of the peak under investigation cannot be found because they are overlaid by another compound. Without any pretreatment of the data, the noise of the baseline is found and integrated as an isotope peak in the middle measurement. This results in a charge count of three for this feature. No isotopic peaks are detected in the first and third measurements, resulting in a feature with a charge number of one and a frequency of two. If a simple moving average in drift and chromatographic dimension is performed over three data points each and removal of all data points below a threshold value of 20 (d3 c3 Min20) prior to the feature analysis, no isotopic peak is found in the middle measurement. Thus, only one feature with a charge number of one and a frequency of three is found.

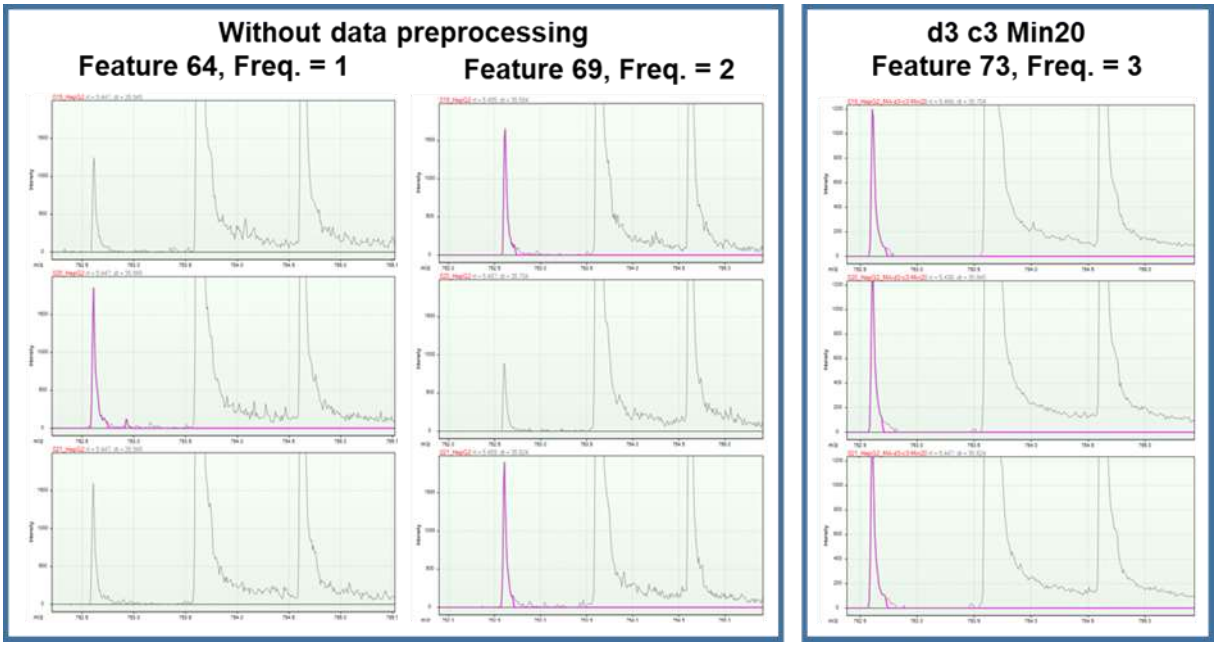

Figure S11: HepG2 lipid extract was analyzed three times by LC-IM-qTOF-MS and feature analysis was performed using Mass Profiler. Mass spectra of a feature are shown. Peaks highlighted in purple were integrated. **Left:** No data pretreatment was performed prior to feature analysis. The isotopic peaks of the feature cannot be found because they are overlaid by another compound. In the middle measurement, noise is identified as a peak and set as an isotopic peak, resulting in a feature charge count of three. Therefore, two features are found, one with a frequency of one and another with a frequency of two. **Right:** Smoothing in drift and chromatography dimensions over three data points each and removing all data points below a threshold of 20 (d3 c3 Min20) removes the noise identified as an isotopic peak and only one feature is found with a frequency of three.

Influence of data pretreatment on feature numbers after blank subtraction

Figure 12 to S14 show the number of features of three lipid extracts of different matrices (left: HepG2 cells, middle: Human blood plasma and right: Human blood serum) analyzed by LC-IM-qTOF-MS after blank subtraction. Different data pretreatment parameters were investigated. For data pretreatment, all data points below a threshold of 20 were removed (Min20), in addition, a simple moving average was performed over three points in the drift (d3 Min20), in the chromatography (c3 Min20), and in the drift and chromatography dimension (d3 c3 Min20). A feature analysis was then performed in each case and the feature counts obtained were plotted by frequency (absolute numbers at the top and percentages at the bottom). A Q-Score of 40 was used and single ion features were reported with a charge state of z = 1. For the blank subtraction features were subtracted in order of their occurrence. Intensities were not considered. In Figure S12, features were removed if they were found in all three blanks. In Figure S13, features were removed if they were found in two of the three blanks. In Figure S14, features were removed if they were found once in any blank. In all cases, relative numbers equal the ones without blank subtraction, and similar trends were observed.

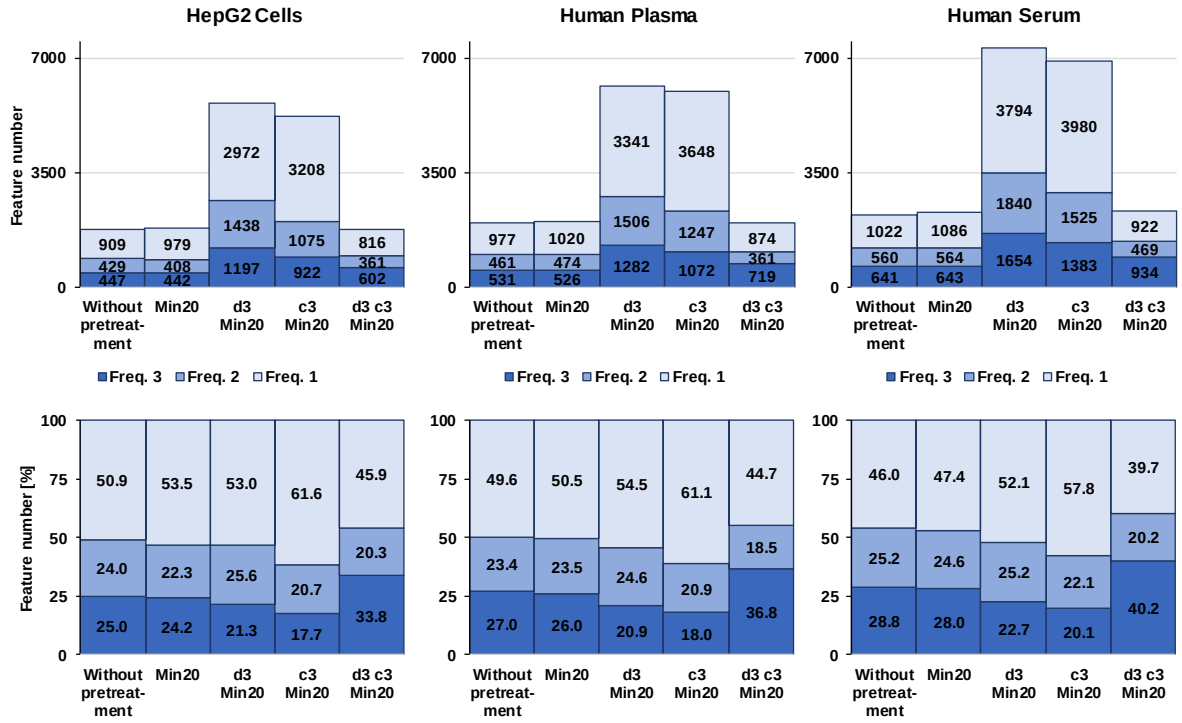

Figure S12: Feature numbers plotted by frequency of different matrices and different data pretreatment before feature analysis and after blank subtraction. Features were removed if they were found in all three blanks.

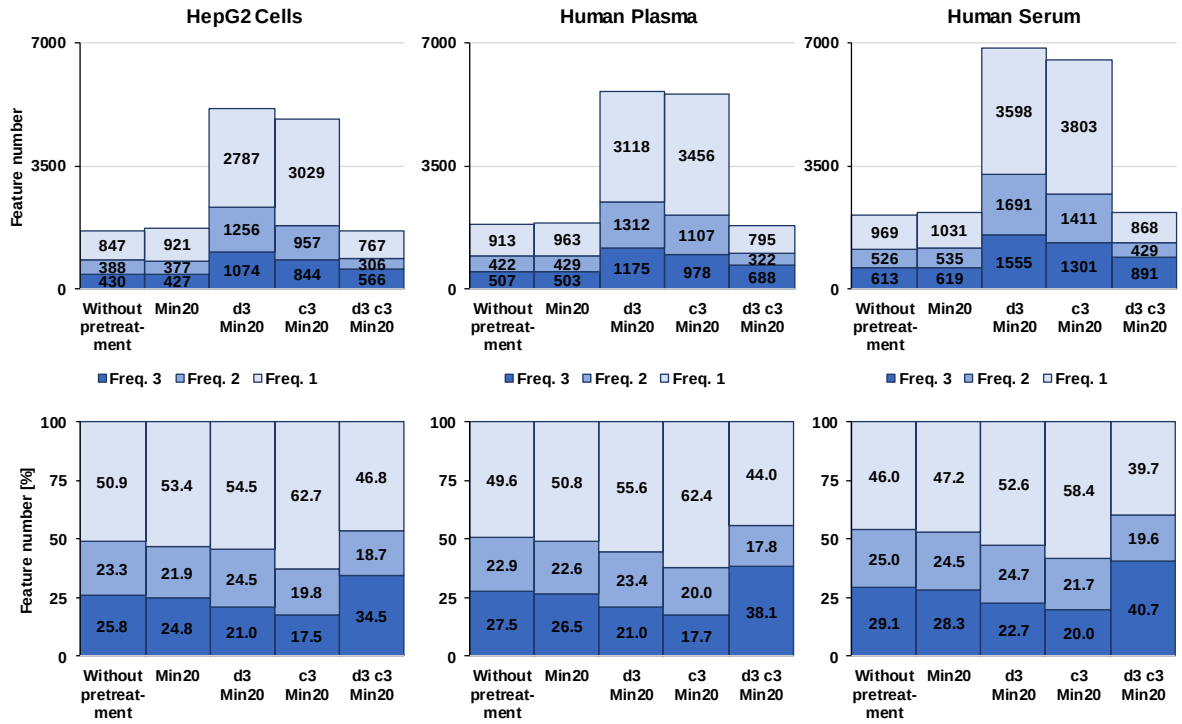

Figure S13: Feature numbers plotted by frequency of different matrices and different data pretreatment before feature analysis and after blank subtraction. Features were removed if they were found in two out of three blanks.

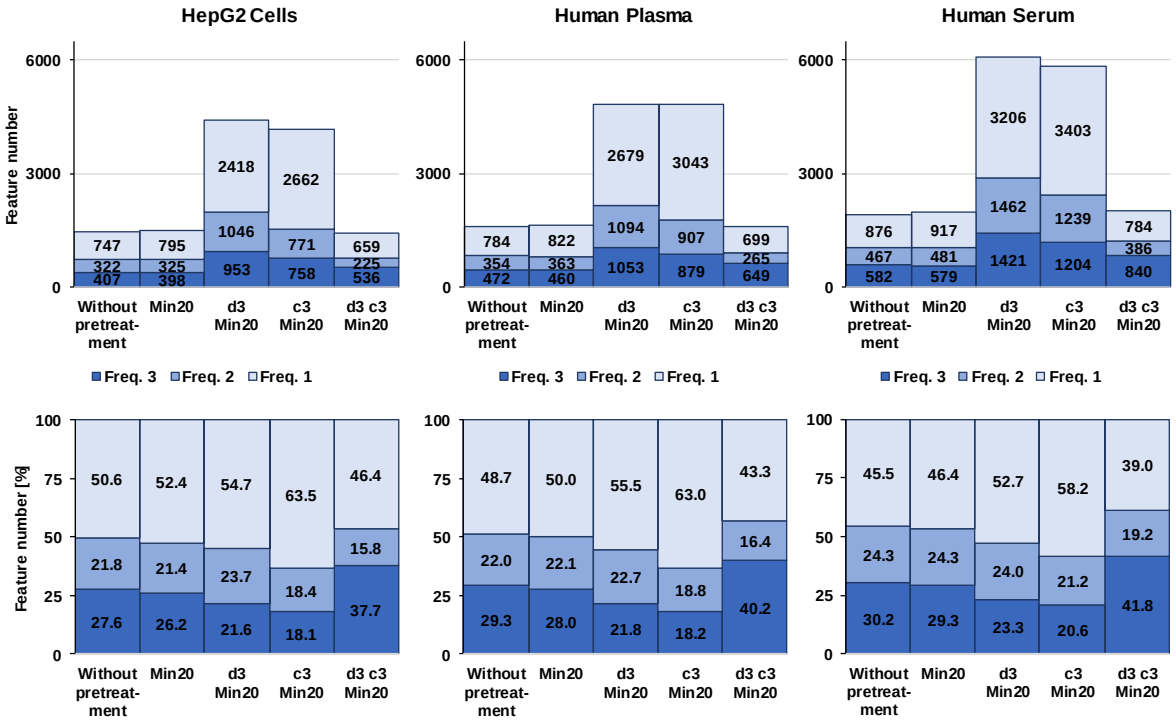

Figure S14: Feature numbers plotted by frequency of different matrices and different data pretreatment before feature analysis and after blank subtraction. Features were removed if they were found once in any blank.

3 References

(1) Bligh, E. G.; Dyer, W. J., A rapid method of total lipid extraction and purification. *Canadian journal of biochemistry and physiology* **1959**, DOI: 10.1139/o59-099.

(2) Gabelica, V.; Shvartsburg, A. A.; Afonso, C.; Barran, P.; Benesch, J. L. P.; Bleiholder, C.; Bowers, M. T.; Bilbao, A.; Bush, M. F.; Campbell, J. L.; Campuzano, I. D. G.; Causon, T.; Clowers, B. H.; Creaser, C. S.; Pauw, E. de; Far, J.; Fernandez-Lima, F.; Fjeldsted, J. C.; Giles, K.; Groessl, M.; Hogan, C. J.; Hann, S.; Kim, H. I.; Kurulugama, R. T.; May, J. C.; McLean, J. A.; Pagel, K.; Richardson, K.; Ridgeway, M. E.; Rosu, F.; Sobott, F.; Thalassinos, K.; Valentine, S. J.; Wyttenbach, T., Recommendations for reporting ion mobility Mass Spectrometry measurements. *Mass spectrometry reviews* **2019**, DOI: 10.1002/mas.21585.

(3) Liebisch, G.; Fahy, E.; Aoki, J.; Dennis, E. A.; Durand, T.; Ejsing, C. S.; Fedorova, M.; Feussner, I.; Griffiths, W. J.; Köfeler, H.; Merrill, A. H.; Murphy, R. C.; O'Donnell, V. B.; Oskolkova, O.; Subramaniam, S.; Wakelam, M. J. O.; Spener, F., Update on LIPID MAPS classification, nomenclature, and shorthand notation for MS-derived lipid structures. *Journal of lipid research* **2020**, DOI: 10.1194/jlr.S120001025.

(4) Kaiser, H.; Specker, H., Bewertung und Vergleich von Analysenverfahren. *Z. Anal. Chem.* **1956**, DOI: 10.1007/BF00454145.

(5) Bowden, J. A.; Heckert, A.; Ulmer, C. Z.; Jones, C. M.; Koelmel, J. P.; Abdullah, L.; Ahonen, L.; Alnouti, Y.; Armando, A. M.; Asara, J. M.; Bamba, T.; Barr, J. R.; Bergquist, J.; Borchers, C. H.; Brandsma, J.; Breitkopf, S. B.; Cajka, T.; Cazenave-Gassiot, A.; Checa, A.; Cinel, M. A.; Colas, R. A.; Cremers, S.; Dennis, E. A.; Evans, J. E.; Fauland, A.; Fiehn, O.; Gardner, M. S.; Garrett, T. J.; Gotlinger, K. H.; Han, J.; Huang, Y.; Neo, A. H.; Hyötyläinen, T.; Izumi, Y.; Jiang, H.; Jiang, H.; Jiang, J.; Kachman, M.; Kiyonami, R.; Klavins, K.; Klose, C.; Köfeler, H. C.; Kolmert, J.; Koal, T.; Koster, G.; Kuklenyik, Z.; Kurland, I. J.; Leadley, M.; Lin, K.; Maddipati, K. R.; McDougall, D.; Meikle, P. J.; Mellett, N. A.; Monnin, C.; Moseley, M. A.; Nandakumar, R.; Oresic, M.; Patterson, R.; Peake, D.; Pierce, J. S.; Post, M.; Postle, A. D.; Pugh, R.; Qiu, Y.; Quehenberger, O.; Ramrup, P.; Rees, J.; Rembiesa, B.; Reynaud, D.; Roth, M. R.; Sales, S.; Schuhmann, K.; Schwartzman, M. L.; Serhan, C. N.; Shevchenko, A.; Somerville, S. E.; St John-Williams, L.; Surma, M. A.; Takeda, H.; Thakare, R.; Thompson, J. W.; Torta, F.; Triebl, A.; Trötzmüller, M.; Ubhayasekera, S. J. K.; Vuckovic, D.; Weir, J. M.; Welti, R.; Wenk, M. R.; Wheelock, C. E.; Yao, L.; Yuan, M.; Zhao, X. H.; Zhou, S., Harmonizing lipidomics: NIST interlaboratory comparison exercise for lipidomics using SRM 1950-Metabolites in Frozen Human Plasma. *Journal of lipid research* **2017**, DOI: 10.1194/jlr.M079012.